

# Mixing of Power-Law Fluids Using Anchors: Metzner-Otto Concept Revisited

S. Murthy Shekhar and S. Jayanti

Dept. of Chemical Engineering, Indian Institute of Technology-Madras, Chennai - 600 036, India

*In 1957 Metzner and Otto proposed a simplified way of calculating the power consumption in impeller-driven systems for power-law type of fluids. Assuming a proportionality between the shear rate and rotational speed of the impeller, they reported that the proportionality constant was independent of the geometric and fluid properties of the mixing system. This was later contested by a number of researchers, and different correlations have been given to evaluate the proportionality constant. An in-depth investigation of the Metzner–Otto concept is discussed with the help of computational fluid dynamics (CFD) techniques to calculate the flow field created by an anchor impeller. Fundamentally, both of the assumptions are broadly valid for typical operating parameters used in anchor-driven impeller systems. A new correlation, based on the Metzner–Otto concept and making use of the present CFD simulations, was developed to calculate power consumption in anchor-driven mixing systems.*

## Introduction

Mixing forms an important unit operation in chemical, pulp, polymer, and other process industries. Many fluids used in these industries are non-Newtonian and typically exhibit shear-thinning characteristics. Due to the high effective viscosity of the fluids, mixing operations are usually done using close-clearance impellers such as anchors, helical ribbons, and helical screws. Design of mixers for these applications is particularly critical from the process economics and the quality of the end-product. Several performance parameters are used to assess the effectiveness of mixers, viz., the power input, mixing and circulation times, and heat-transfer rate across the vessel wall. A number of studies of the various impeller characteristics have been reported in the literature; useful reviews have been given in Nagata (1975) and Harnby et al. (1985). The present study is focused on anchor impellers, which are widely used in applications involving heat transfer.

Early studies of mixing using close-clearance impellers necessarily have been experimental, as the flow field produced by these is fairly complicated and cannot be predicted from purely analytical studies. These studies showed that power consumption is characterized primarily by the impeller Reynolds number,  $Re$ , defined as  $d^2 N \rho / \mu$ , where  $\rho$  is the

density,  $d$  is the diameter of the impeller,  $N$  is the rotational speed of the agitator in revolutions per second, and  $\mu$  is the dynamic viscosity. Typically, for anchor impellers, the flow is laminar for  $Re < 10$ , transitional for  $10 < Re < 300$ , and turbulent for higher Reynolds numbers (Nagata, 1975). In the laminar regime, the power consumption, represented by the power number,  $Po$ , defined as  $P / \rho N^3 d^5$ , where  $P$  is the power, is inversely proportional to the impeller Reynolds number, and it becomes progressively less sensitive as  $Re$  increases, as indicated by the data of Calderbank and Moo-Young (1961), among others. The proportionality constant between  $Po$  and  $1/Re$  depends on a number of geometric parameters including the clearance between the impeller tip and the vessel wall, and the height and width of the impeller blade (Calderbank and Moo-Young, 1961; Beckner and Smith, 1966; Shamlou Ayazi and Edwards, 1989). For non-Newtonian flows, the studies have been confined mainly to power-law type of fluids and the studies just mentioned showed considerable influence of the fluid behavior index,  $n$ . It was noted that for shear-thinning liquids, the smaller the numerical value of  $n$ , the lower was  $Po$ , while the converse was true for shear-thickening fluids (Tanguy et al., 1996).

While the prediction of  $Po$  poses no special problems for Newtonian fluids, the situation is somewhat different for power-law fluids, because the effective viscosity, which is

Correspondence concerning this article should be addressed to S. Jayanti.

needed for the evaluation of the impeller Reynolds number, is a function of the shear rate, which itself is a function of the flow parameters. One approach that is often adopted (Calderbank and Moo-Young, 1961; Beckner and Smith, 1966) is to modify the definition of the Reynolds number such that the viscosity of the fluid does not appear explicitly. For example, Calderbank and Moo-Young (1961) correlated their data of power consumption in terms of a Reynolds number defined as

$$Re' = \frac{d^2 N \rho (BN)^{1-n}}{K} \left( \frac{4n}{3n+1} \right)^n \quad (1)$$

where  $K$  is the consistency index,  $n$  is the flow behavior index, and  $B$  is a dimensionless constant. Similarly, Beckner and Smith (1966) used

$$Re'' = \frac{d^2 N^{2-n} \rho}{K [a(1-n)]^{n-1}} \quad (2)$$

where  $a$  is an empirical constant given in terms of the clearance ratio,  $c/T$ , as

$$a = 37 - 120 \frac{c}{T} \quad (2a)$$

where  $c$  is the clearance between impeller blade and vessel wall and  $T$  is the diameter of the vessel. In both of these above definitions, the effective Reynolds number for a power-law fluid, viz.,  $d^2 N^{2-n} \rho / K$  is modulated by an empirical parameter that depends on geometrical characteristics of the impeller and the vessel as well as by the fluid behavior index,  $n$ .

An alternative approach to the correlation of the power consumption for non-Newtonian fluids, and one that is being increasingly adopted by a number of researchers (Rieger and Novak, 1973; Sestak et al., 1986; Shamlou Ayazi and Edwards, 1989) is the use of a Reynolds number based on the effective or apparent viscosity. Here, the Reynolds number is defined as

$$Re = d^2 N \rho / \mu_a \quad (3)$$

where  $\mu_a$ , the apparent viscosity, is made to depend on the geometrical and flow characteristics. This approach was originally proposed by Metzner and Otto (1957) and has the advantage of adapting the  $Po$  vs.  $Re$  relation for a Newtonian fluid to power-law fluids. Thus, a single correlation of  $Po$  in terms of  $Re$  and the geometrical characteristics would be sufficient for all Newtonian and power-law fluids, unlike in the case of the modified Reynolds number approach where the correlation would be fluid-specific in addition to being geometry-specific. However, the success of this type of correlation would depend on the accurate estimation of the apparent viscosity. Since the rheological behavior of the power law is given in terms of  $n$  and  $K$ , this implies that the determination of the effective shear rate ( $\dot{\gamma}$ ) to go into the apparent viscosity relation

$$\mu_a = K (\dot{\gamma})^{n-1} \quad (4)$$

is crucial. Here, Metzner and Otto (1957) suggested, based on their studies of flat-bladed turbine impellers, that the effective shear rate in the general region of the impeller could be taken as being directly proportional only to the speed of rotation of the impeller. They, thus, expressed the effective shear rate as

$$\dot{\gamma} = K_s N \quad (5)$$

For the range of parameters in their study, they proposed a value of 13 for the proportionality constant  $K_s$  and reported good agreement with a Newtonian fluid correlation between  $Po$  and  $Re$  for a range of power-law fluids with this value for  $K_s$ . This Metzner–Otto concept was adopted by a number of later researchers to correlate their power-consumption results for anchor and other close-clearance impellers. However, a wide range of values of the proportionality constant,  $K_s$ , have been reported, including a theoretical value of  $4\pi (= 12.56)$ ; close to the value of 13 proposed by Metzner and Otto), treating the flow in an anchor-driven vessel to similar to the Couette flow between rotating concentric cylinders. Table 1 contains a listing of this and other values and correlations available in the literature to determine the value of  $K_s$ . Interestingly,  $K_s$  is found to vary not only with geometrical parameters but also with the flow behavior index,  $n$ .

**Table 1. Values of  $K_s$  Reported in the Literature**

Source	$c/T$	$n$	$K_s$
Pollard and Kantyka (1969)	0.0834	0.35–0.78	18
Nagata (1975)	0.05	0.2–0.8	25
Beckner and Smith (1966)	0.02–0.1057	0.29–0.73	$K_s = a(1-n)$ $a = 37 - 120(c/T)$
Calderbank and Moo-Young (1961)	0.05	0.05–1.87	$K_s = \left[ 9.5 + \frac{9(T/d)^2}{(T/d)^2 - 1} \right] \left( \frac{3n+1}{4n} \right)^{n(n-1)}$
Schilo (1969)	0.05, 0.024	0.5, 0.54	$K_s = \left[ \frac{(4\pi)^{n-1} (T/d)^2 - 0.75}{n^n [(T/d)^{2/n} - 0.75]^n} \right]^{1/(0.9(n-1))}$
Sestak et al. (1986)	0.05	0.07–1.0	$K_s = 35^{[n/(1-n)]}$
Rieger and Novak (1973)	0.05	—	$K_s = n^{[2.2/(n-1)]}$
Shamlou Ayazi and Edwards (1989)	0.0225–0.123	0.2–0.75	$K_s = 33 - 172(c/T)$
Tanguy et al. (1996)	0.05	0	$25 \pm 2$

However, contradictory results have been reported on both counts. For example, Shamlou Ayazi and Edwards (1989) have reported that  $K_s$  is a function only of the geometric parameters and not of the flow behavior index. In contrast, Beckner and Smith (1966) deduce from their data that  $K_s$  is indeed a function of the flow behavior index. Both Rieger and Novak (1973) and Sestak et al. (1986) also present correlations for  $K_s$  in terms of  $n$ .

Recently, Tanguy et al. (1996) conducted a numerical study of the flow field in an anchor-driven vessel with fixed geometric parameters, except for different power-law fluids in the flow behavior index range of 0.3 to 1.7. They deduced the value of  $K_s$  from the power calculations for a Newtonian and a power-law fluid and found it *not* to be a strong function of the flow behavior index. However, the studies of Tanguy et al. were limited to one geometric configuration only. Also, they derived the value of  $K_s$  indirectly from the ratio of the product ( $Po \cdot Re$ ) for a power-law fluid to that for a Newtonian fluid. In view of this, and in view of the advantages offered in a numerical simulation—being able to fix accurately the values of  $n$  and  $K$  of a power-law fluid (which are usually found to vary from experimenter to experimenter for the same nominal fluid), and being able to calculate the local velocity field and shear rates throughout the vessel for a given set of global conditions—a computational-fluid-dynamics-based (CFD) approach has been adopted in the present article to study this problem. To this end, numerical simulations of the flow induced by an anchor impeller have been carried out over a range of operating parameters for typical anchor systems. The predicted velocity field and the computed overall power consumption data have been analyzed to examine the validity of the assumptions underlying the Metzner–Otto concept. It is shown that over the range of parameters investigated, the major assumption of a constant  $K_s$  that is independent of geometric and fluid parameters is largely valid. Based on the present simulations of about 70 cases, a correlation for the power number has been constructed with the assumption of constant  $K_s$ , and it is shown to predict data found in the literature with as good accuracy as some of the well-known correlations for anchor impellers. The methodology of this study and the results obtained leading to the preceding conclusions are discussed below.

## Methodology and Problem Formulation

### Basic equations

The design of an agitator for a mixing system is usually based on empirical correlations for mixing, heat transfer, and power consumption. The advent of CFD techniques in recent years has made it possible to investigate the details of the complicated flow field generated by the impellers (Bernard and Coudrec, 1988; Tanguy et al., 1992; Kaminoyama et al., 1993). The usual approach taken in CFD simulations is to use finite-element/finite-volume methods to take account of the complicated shape of the impeller. In the present study, a finite-volume-method-based simulation is presented for the mixing of Newtonian and non-Newtonian fluids using anchor blades. The calculations are done using the commercial code CFX developed by AEA Technology, U.K.

The basic equations solved in mixing calculations are those describing the flow of fluids viz., conservation of mass, mo-

mentum and energy. The fluids are considered to be incompressible. For non-Newtonian fluids, the viscosity of the fluid depends on the shear rate experienced by the fluid, and a power-law fluid model (Bird et al., 1960) is used in the present study. Accordingly, the viscous stress vs. strain-rate relation is given by the following equation for a general three-dimensional motion

$$\tau = \left\{ K \left| \sqrt{\frac{1}{2}(\Delta:\Delta)} \right|^{n-1} \right\} \Delta \quad (6)$$

where  $\Delta$  is the deformation-rate tensor. The flow is taken to be laminar in all cases, and the maximum impeller Reynolds number studied in the simulations was 23. Hence, no turbulence model is used in the calculations.

### Representation of the impeller

A number of strategies can be employed to deal with the movement of the impeller blades. These include (1) use of momentum source term (Xu and McGrath, 1996), (2) solving the governing equations in a rotating coordinate system (Harvey et al., 1997), and (3) sliding-mesh approach (Bakker et al., 1997). Of these, the sliding mesh method is the most versatile and is used in the present study. The details of the sliding-mesh technique are available in the literature (Murthy et al., 1994). The basic idea is to employ two grids, one of which moves with the impeller while the other is fixed to the tank. The meshes interact along a surface of slip, and the moving grid is allowed to slide relative to the stationary one. The grid lines are not required to align themselves on the slip surface; a conservative interpolation is used to obtain the flow variables and face fixed across this surface. The principal feature of the sliding-mesh method is that the flow field over the impeller is resolved as part of the solution, and, hence, no specification other than the geometrical details is necessary to represent the impeller. Thus, no empiricism is introduced in representing the impeller motion.

### Estimation of power consumption

The fact that the flow field around the impeller is resolved enables the estimation of the power directly from a calculation of the total torque required to rotate the impeller. Since the flow domain as well as the enveloping surface is subdivided into small volumes and areas as part of the CFD solution, the shear stress and the pressure distribution on the impeller blade become available at the end of the calculation, that is, once a steady state is reached. The torque,  $T$ , on each blade can be readily calculated as

$$T = \sum_i (\Delta p)_i A_i r_i \quad (7)$$

where the summation is carried over all the cells having the blade as one of the boundaries. Here,  $\Delta p$  is the pressure difference between the front (upstream) and the back (downstream) side of the blade at the surface element  $i$ ,  $A_i$  is the projected surface area of the surface element  $i$ , and  $r_i$  is the radial distance from the axis of the shaft on which the impeller is mounted. The power required for rotation of the

impeller at a steady rotational speed of  $N$  revolutions per second for an impeller having  $n_b$  blades is then given by

$$P = 2\pi N n_b T \quad (8)$$

from which the power number,  $Po$ , is calculated as  $P/(\rho N^3 d^5)$ .

### Details of simulations

All the calculations were done using the commercially available CFX computer code developed by AEA Technology, UK. CFX is a general-purpose computer program using a finite-volume method based discretization on a nonstaggered grid using the Rhie–Chow algorithm (Rhie and Chow, 1983) to avoid checkerboard oscillations associated with the use of nonstaggered grids. In the present study, a third-order accurate quadratic upwind differencing (QUICK) scheme was used for discretization of convective flux terms.

The system consists of a cylindrical vessel of diameter 0.228 m with an anchor impeller of a given diameter and a width of 0.024 m. The impeller was located at a distance of 0.016 m from the bottom of the vessel. The height of the liquid was maintained to be the same as the tank diameter, that is, 0.228 m. The free surface at the top of the vessel was treated as a flat, shear-free boundary. The impeller shaft was concentric with the axis of the vessel. The problem has been formulated in cylindrical coordinates with three dimensions, the axial, radial, and tangential components being  $u$ ,  $v$ , and  $w$ , respectively. Due to symmetry of the impeller and vessel, calculations were performed for a sector of  $180^\circ$  (Figure 1), and pe-

riodic boundary conditions were imposed in the circumferential directions at the two ends of the sectors. A  $114 \times 57 \times 12$  grid in the axial, radial, and circumferential (covering only  $180^\circ$ ) directions was used to discretize the flow domain. In order to verify the fineness of the grid, additional calculations were done with a  $114 \times 57 \times 24$  grid (doubling the number of grid points in the circumferential direction) as well as with a  $228 \times 114 \times 24$  grid. Significant differences were not found in the calculated velocity profiles. Since the computational time memory requirements for these time-dependent calculations were very high in these simulations, especially in the last case, the  $114 \times 57 \times 12$  grid was used in all subsequent calculations.

The calculations were started with a zero initial velocity condition and were advanced in time with a time step corresponding to a  $15^\circ$  rotation of the impeller. The local and average values of the velocities and stresses were monitored to determine whether or not a steady state was reached. Typically, about 1500 time steps, corresponding to about 60 revolutions of the impeller, were required to achieve a steady, cyclical variation of the flow variables. The power number ( $Po$ ) was then calculated from the pressure distribution on the impeller.

The velocity field and power calculations correspond to the experimental details given in Beckner and Smith (1966). In order to investigate the effect of clearance on the performance, additional calculations have been done for other geometric configurations as listed in Table 2a. For these geometrical characteristics, calculations of power were carried out at different impeller speeds and with four different fluids. The relevant properties of the fluids are listed in Table 2b. Results from these simulations are discussed below.

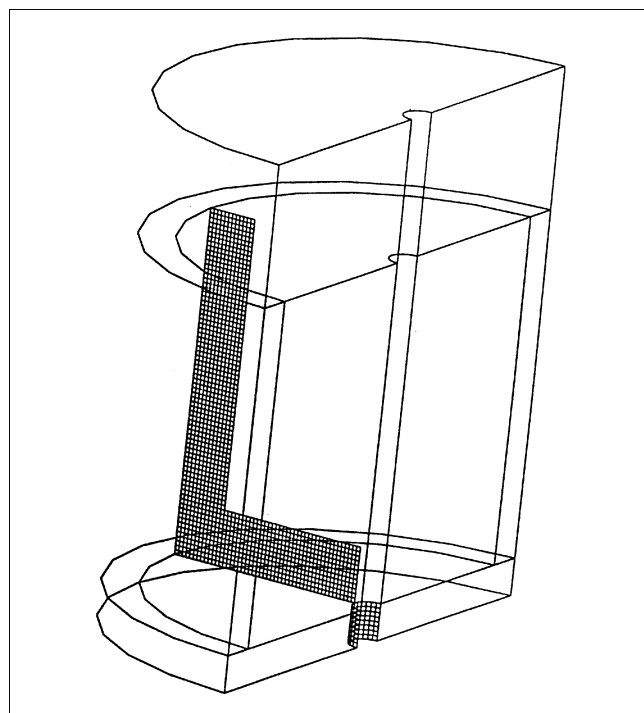


**Figure 1. Geometry of the flow domain for simulations showing one-half of the anchor impeller (hatched portion) and the cylindrical vessel.**

## Results and Discussion

The results from the preceding computations are presented in three parts. In the following subsection, the computed velocity field and the predicted power number are compared with existing data in the literature to demonstrate the accuracy of the computations. In the subsection on the Metzner–Otto concept for anchor impellers, the computed

**Table 2.**

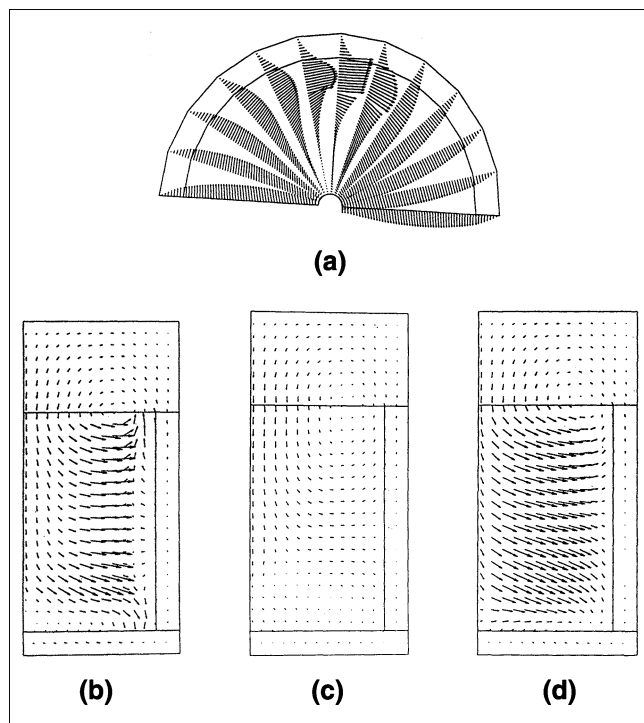
(a) Geometrical Details of the Mixing Systems in the Present Study					
Case No.	Dia. of Vessel, $T$ (m)	Dia. of Impeller, $d$ (m)	Height of Impeller, $h$ (m)	Width of Impeller, $w$ (m)	Clearance, $c/T$
1	0.228	0.216	0.15	0.024	0.026
2	0.228	0.196	0.15	0.024	0.070
3	0.228	0.180	0.15	0.024	0.105

(b) Rheological Properties of Fluids Used in the Present Study				
Case No.	Liquid	Density, $\rho$ (kg/m <sup>3</sup> )	Consistency Index, $K$ , (Pa·s)	Flow Behavior Index, $n$
1	Silicone liquid	980	0.567	1.0
2	10% aq. CMC*	1043	176.3	0.266
3	9.46% aq. CMC	1053	56.7	0.469
4	Diluted PBD**	804	93.4	0.766

\* Carboxymethyl cellulose.

\*\* Polybutadiene dissolved in ethylbenzene.



**Figure 2. Calculated velocity vectors (projected onto the plane in which they are plotted) for a Newtonian fluid at a Reynolds number of 9.4 for the geometrical details of Case 2 in Table 2a.**

(a) In a horizontal plane at the midway height of the impeller, (b) in a vertical plane at  $\theta = 0^\circ$  (corresponding to the impeller plane), (c) in a vertical plane at  $\theta = 90^\circ$ , and (d) in a vertical plane at  $\theta = 150^\circ$ .

velocity field is analyzed to examine how far the assumptions of Metzner and Otto (1957) are valid. In the subsequent subsection, a correlation for the power number is proposed based on the present results and is compared with data and correlations in the literature.

### Flow field and power consumption

A typical velocity field obtained in the calculations is shown in Figure 2 for a Newtonian fluid at a Reynolds number of 9.4, which corresponds to the experimental results given in Beckner (1965). In Figure 2a, the velocity vectors (projected onto the plane in which they are plotted) are plotted in a horizontal plane at a section midway along the impeller, while the velocity vectors at  $\theta = 0^\circ$  (corresponding to the impeller plane),  $90^\circ$ , and  $150^\circ$  are shown in Figures 2b, 2c, and 2d, respectively. (For the sake of clarity, velocity at all grid points is not shown and the grid is much finer than what is implied in these figures.) It can be seen that the flow is primarily circumferential, and although axial mixing can be seen in Figures 2b, 2c, and 2d, the associated circulation velocity is rather small. The maximum axial velocity is typically on the order of 5% of the tip speed for an  $Re$  of 10, and is much less at lower  $Re$ . It can also be seen that while a circumferential flow is created throughout the vessel, the velocity field near the impeller is quite different. This indicates that the flow

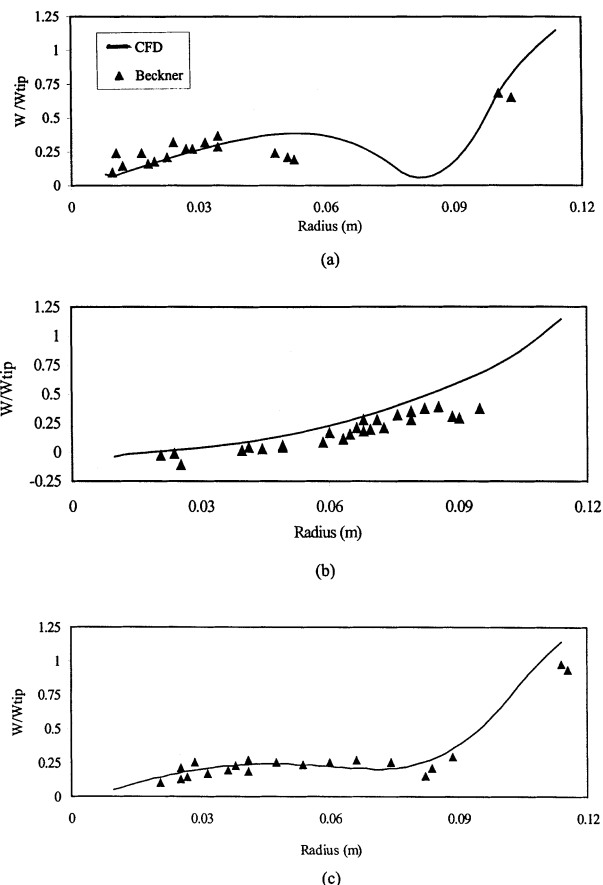


**Figure 3. Comparison with the data of Beckner (1965) of the circumferential velocity component at (a)  $\theta = 0^\circ$ , (b)  $\theta = 90^\circ$ , and (c)  $\theta = 150^\circ$  for the case in Figure 2.**

field is never steady, but that it ultimately reaches a periodic steady state. As indicated earlier, it typically takes about 60 revolutions of the impeller to achieve this state from a stagnant flow condition.

The predicted circumferential velocity profiles are compared in Figure 3 with those measured by Beckner (1965) as given in Peters and Smith (1967) at three circumferential positions. It can be seen that fairly good agreement is obtained between the two. The power computed according to Eqs. 7 and 8 is converted into  $Po$  and is plotted as a function of the Reynolds number in Figure 4 for Case 2 of Table 2a, that is, for an impeller with a clearance ratio of 0.075. Also shown in this plot are the predicted  $Po$  according to the correlations of Beckner and Smith (1966) given by

$$Po = 82 \left[ \frac{Nd^2\rho}{\mu} \right]^{-0.93} \left[ \frac{c}{T} \right]^{-0.25} \quad (9)$$

and of Shamlou Ayazi and Edwards (1989) given by

$$Po = 8.5\pi^3 n_b \left[ \frac{Nd^2\rho}{\mu} \right]^{-1} \left[ \frac{h}{d} \right] \left[ \frac{w}{d} \right] \left[ \frac{c}{T} \right]^{-0.5} \quad (10)$$

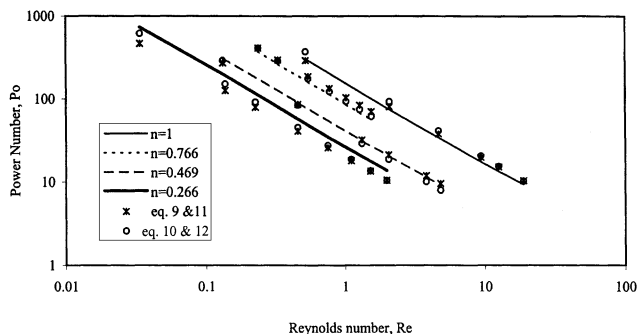


**Figure 4.** Power number ( $Po$ ) predicted by the present simulations (lines) vs. those obtained from empirical correlations of Beckner and Smith (1966) (denoted by asterisks) and Shamlou Ayazi and Edwards (1989) (denoted by open circles) for Newtonian and power-law fluids at various Reynolds numbers for the Case 2 of Table 2a.

where  $n_b$  is the number of blades ( $= 2$  for anchor impellers),  $h$  is the height, and  $w$  the width of the impeller. It can be seen that excellent agreement is obtained between the predictions based on the present CFD calculations and those

from empirical correlations. Similar agreement is also obtained for the two geometrical cases (Case 1 and Case 3 of Table 2a) considered in the present study.

For the case of non-Newtonian fluids, no data are available for the comparison of the velocity field. Data of power are available in the form of correlations such as those given in Eqs. 9 and 10 extended to cover power-law fluids. As a further validation of the present computations, the predicted power for the various non-Newtonian fluid combinations given in Table 2b are plotted in Figure 4 as a function of  $Re$  defined here as  $(d^2 N^{2-n} \rho / K)$  for the geometrical parameters corresponding to Case 2 of Table 2a. Also shown here are the predictions of the correlation of Beckner and Smith (1966) for non-Newtonian fluids given by

$$Po = 82 \left\{ \frac{d^2 N^{2-n} \rho}{K [a(1-n)]^{n-1}} \right\}^{-0.93} \left\{ \frac{c}{T} \right\}^{-0.25} \quad (11)$$

where

$$a = 37 - 120 \frac{c}{T} \quad (11a)$$

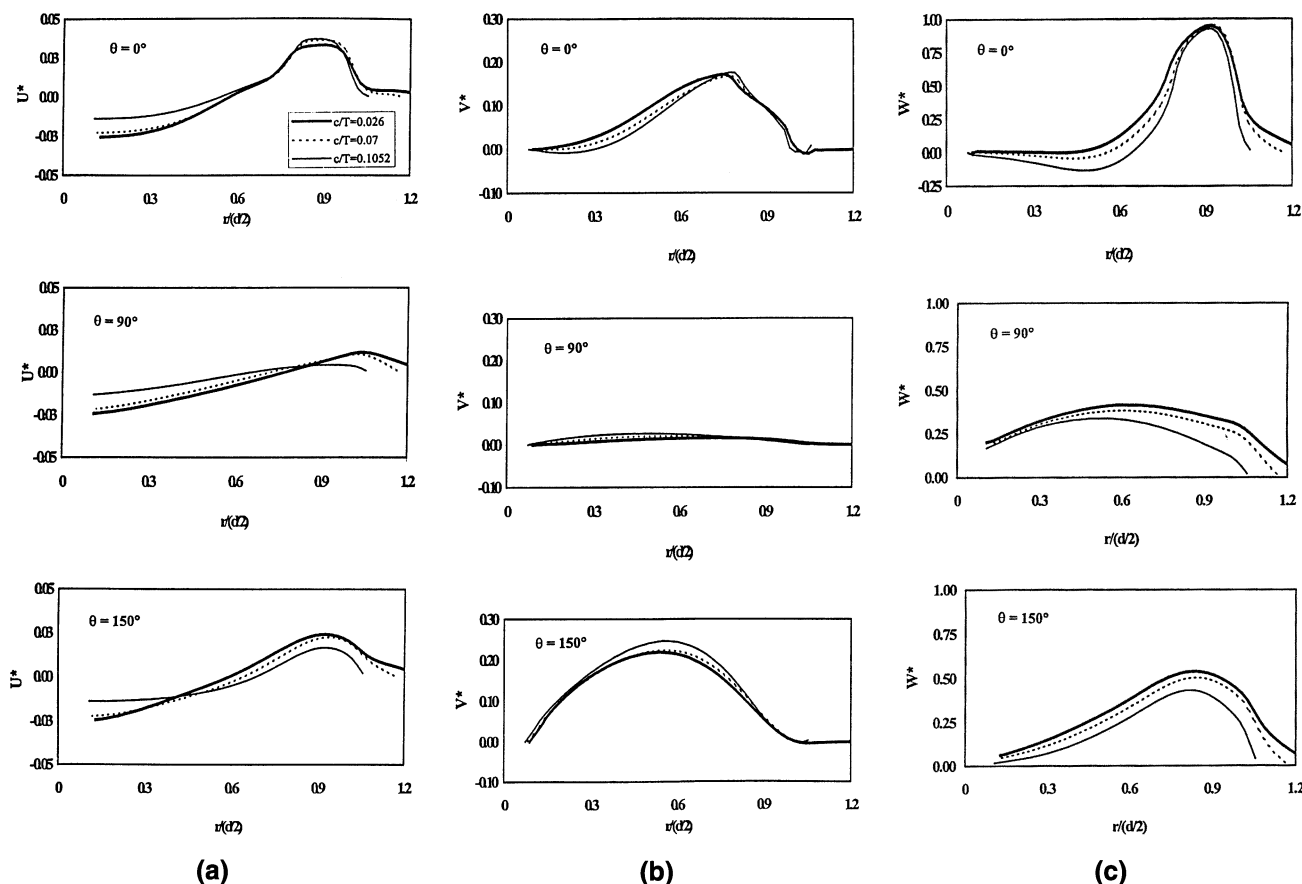


**Figure 5.** Variation of velocity components with the clearance ratio for a flow behavior index of 0.469 at  $\theta = 0^\circ$ ,  $90^\circ$ , and  $150^\circ$ : (a) axial velocity component, (b) radial velocity component and (c) circumferential velocity component.

and of Shamlou Ayazi and Edwards (1989) given by

$$Po = 8.5\pi^3 n_b \left[ \frac{Nd^2p}{\mu_a} \right]^{-1} \left[ \frac{h}{d} \right] \left[ \frac{w}{d} \right] \left[ \frac{c}{T} \right]^{-0.5} \quad (12)$$

where the Reynolds number is defined based on an apparent viscosity (Eq. 4), with the shear rate in Eq. 5 being calculated using the following correlation for the proportionality constant

$$K_s = 33 - 172 \frac{c}{T} \quad (12a)$$

The results given in Figure 4 show that for all the fluid combinations, the agreement between the predictions of the correlations and those of the CFD simulations is very good. There is a similar level of good agreement between CFD predictions and those based on empirical correlations for the other two geometrical combinations listed in Table 2a. Taken together, these results demonstrate that good agreement of power for non-Newtonian fluids can be obtained using CFD simulations requiring no empirical input. In the present context, they can also be interpreted as providing validation for the power-law fluid calculations. This is important, because the computed CFD results can now be analyzed to see the validity of the Metzner–Otto concept, as described below.

#### **Metzner–Otto concept for anchor impellers**

Metzner and Otto (1957) studied the power-consumption pattern for power-law fluids using a flat-bladed turbine impeller and suggested that the shear rate near the impeller, which is required in order to evaluate the effective viscosity for the computation of an effective Reynolds number so that the power consumption can be determined, was directly proportional to the speed of rotation and that this proportionality constant,  $K_s$ , was largely independent of the flow behavior index. This would, therefore, permit the use of a Newtonian power correlation for a given impeller to estimate the power for a non-Newtonian fluid, provided the value of  $K_s$  was known. It has been suggested in the literature that the value of  $K_s$  was constant; that it was a function of the geometric parameters only; and that it was a function of both geometric parameters and the flow behavior index. These conclusions, or to be exact, the correlations for  $K_s$ , were arrived at based on overall power prediction only. In the present case, since the entire flow field is available, it is possible to examine whether or not the hypothesis is intrinsically correct, that is, whether or not a value of the  $K_s$  derived from the *local shear rate near the impeller* is independent of the geometric and fluid parameters. Since several experimental studies point to the preponderance of the clearance ratio,  $c/T$ , among the geometric parameters and of the flow behavior index,  $n$ , among the fluid properties in determining the power consumption, the focus of the present investigation is confined only to these two parameters. It is noted that the variation of these parameters in the simulations (see Tables 2a and 2b) in practice covers the typical range of application of anchor impellers.

Before we examine the CFD-derived  $K_s$  values, it is necessary to take account of the typical variation of the velocity

field with these parameters. This is summarized in Figures 5 and 6, where the profiles of the velocity components at the midheight of the impeller are shown at three circumferential positions corresponding to  $\theta = 0^\circ$ ,  $90^\circ$ , and  $150^\circ$ . The variation of the velocity components with the clearance ratio is shown in Figure 5 for a flow behavior index of 0.469, while their variation with the flow behavior index is shown in Figure 6 for a clearance ratio of 0.07. In all of the cases, the impeller Reynolds number is about 1, although not exactly so. In these plots, the velocity is nondimensionalized by dividing it by the tip velocity, as is the radial position by dividing it by the impeller diameter. It can be seen in Figure 6 that the profiles of the velocity components at each  $\theta$ -plane are fairly similar for the three  $c/T$  ratios. The profiles for a  $c/T$  ratio of 0.1052 are obtained at a Reynolds number of 1.11, while for the other two, the Reynolds number was 1.32. This may cause some of the systematic variation for the three  $c/T$  ratios seen in Figure 5.

The effect of the flow behavior index can be seen in Figure 6, where the nondimensionalized velocity profiles are plotted for a  $c/T$  ratio of 0.07 and at flow behavior indices of 1 (at a Reynolds number of 1.05), 0.766 ( $Re = 1.28$ ), 0.469 ( $Re = 1.33$ ) and 0.266 ( $Re = 1.11$ ). It can be seen that the velocity profiles are fairly sensitive to the value of the flow behavior index in the bulk of the flow and show a regular trend with decreasing  $n$ . However, the principal component of the flow field, namely, the circumferential velocity component, is relatively unaffected by variation in  $n$ , especially near the impeller.

The variation in the calculated shear rate with flow and geometric parameters can now be examined. Typically, as shown in Figure 7, the shear rate varies widely in the vessel and the effective (apparent) viscosity varies by three orders of magnitude within the vessel. However, close to the impeller, the situation is somewhat similar to what is hypothesized by Metzner and Otto (1957). The shear rate near the impeller [taken here as the volume-weighted, circumferentially averaged (to take the periodicity of the flow into account) value of the shear rate in the cells immediately adjacent to the impeller surface over the entire length of the impeller] exhibits a linear relation with the rotational speed for different values of  $c/T$  (Figure 8a) and for different values of  $n$  (Figure 8b). This linear variation is to be expected from the velocity field, as the principal velocity component is the circumferential velocity, which is roughly proportional to the speed of rotation. From plots such as these, it is possible to calculate the  $K_s$  value for each combination of  $c/T$  and  $n$ . These values of  $K_s$  are plotted in Figure 9 as a function of the flow behavior index. Also shown here are the predicted values of  $K_s$  from the empirical correlations of Beckner and Smith (1966) and Shamlou Ayazi and Edwards (1989), whose correlations are given by Eqs. 11a and 12a, respectively. It can be seen that the CFD-calculated value of  $K_s$  for the three  $c/T$  ratios and for the four fluid behavior index values is roughly constant. This validates the assumption of Metzner and Otto (1957) that the proportionality constant is fairly independent of both these parameters.

It is interesting to note that the  $K_s$  value computed from the correlation of Beckner and Smith shows a significant variation (compared to the CFD value) with both  $c/T$  and  $n$ . The value predicted from the Shamlou Ayazi and Edwards

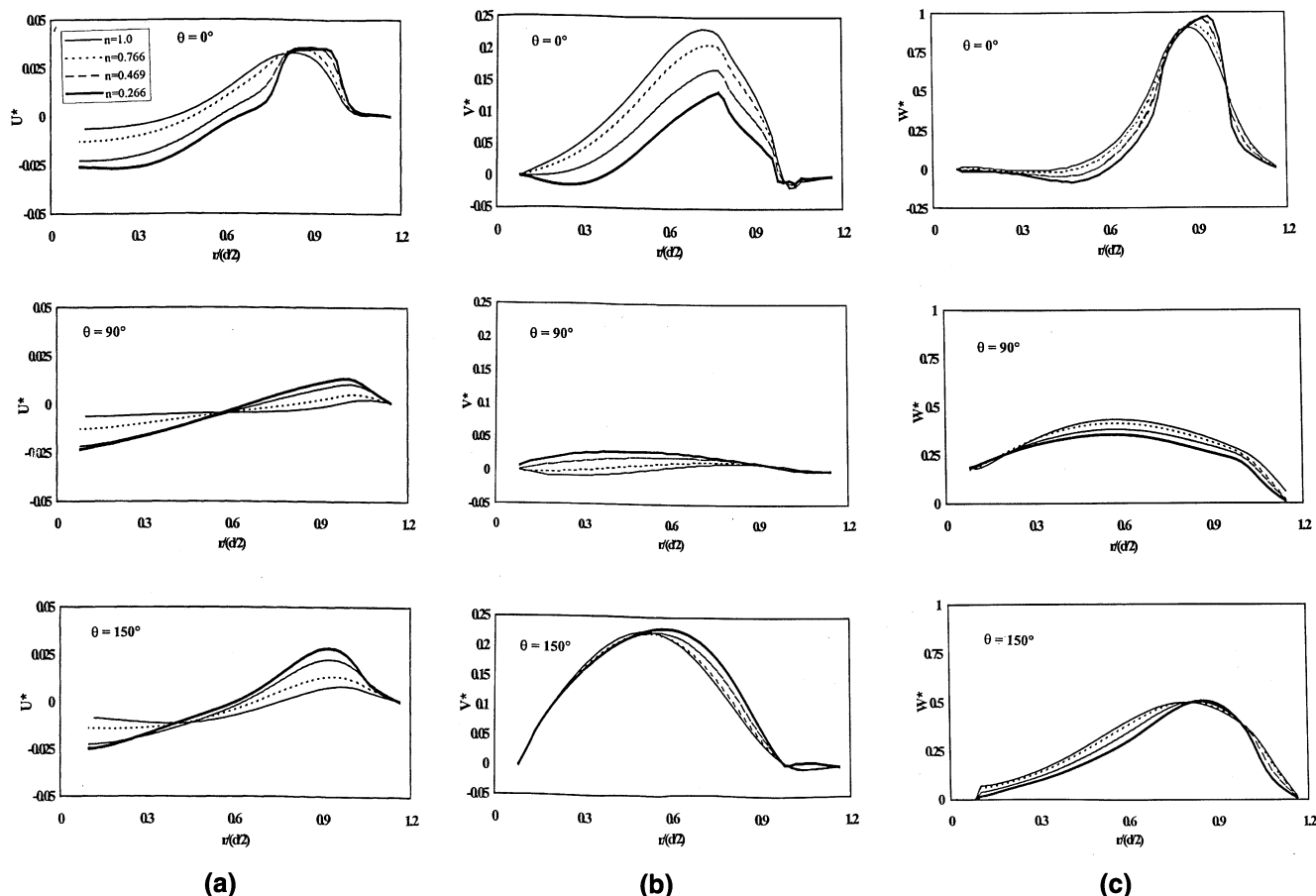


**Figure 6.** Variation of velocity components with the flow behavior index for a clearance ratio of 0.070 at  $\theta = 0^\circ$ ,  $90^\circ$ , and  $150^\circ$ : (a) axial velocity component, (b) radial velocity component, and (c) circumferential velocity component.

correlation does not show any variation with  $n$ , but is significantly affected by the  $c/T$  ratio. However, the three correlations and these computed and correlated values give rise to a power prediction that is typically as good as that shown in Figure 4. This goes to show that a power-consumption correlation can be developed to have any variation of  $K_s$ ; the form of the correlation would be different in each case. This can also explain the wide variation of  $K_s$  (see Table 1) reported in the literature. The present numerical results showing nearly constant  $K_s$  imply that it may be possible to incorporate the geometry effect into the power correlation for a Newtonian fluid, and similarly incorporate the flow behavior index effect into the definition of the Reynolds number. The development of such a correlation is described in the next subsection.

#### Correlation for power consumption for anchor impellers

Experimental and theoretical studies have shown that for anchor impellers

$$Po = f_1(Re, c/T, n) \quad (13)$$

which can be written in several alternate forms, such as

$$Po = f_2(Re, K_s); \quad K_s = f_3(c/T, n) \quad (14a)$$

$$Po = f_4(Re, K_s, c/T); \quad K_s = f_5(n) \quad (14b)$$

$$Po = f_6(Re, K_s, n); \quad K_s = f_7(c/T) \quad (14c)$$

For example, Beckner and Smith (1966) presented a correlation of the form of Eq. 14a; Sestak et al. (1986) presented a correlation of the form of Eq. 14b, and Shamlou Ayazi and Edwards (1989) of the form of Eq. 14c. The present numerical results described in the preceding subsection show that the  $K_s$  derived directly from the variation with a rotational speed of the shear rate near the impeller is nearly independent of the principal geometric parameter,  $c/T$ , and the flow behavior index,  $n$ . Since the power requirement from the CFD simulations matched well with that predicted by correlations from the literature, it may be possible to develop a power correlation based on the Metzner–Otto concept of the form

$$Po = f(\rho N^{2-n} d^2 / K K_s^{(n-1)}, c/T, K_s); \quad K_s = \text{constant} \quad (15)$$

which would be valid for both Newtonian and power-law fluids. Based on the numerical studies that gave a value of  $K_s$  of about 12 and taking note of the theoretical value of  $4\pi$  for a Couette-flow type of model for anchors and also of the



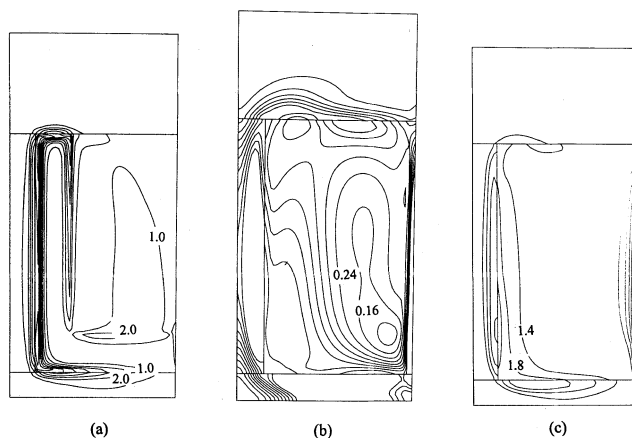


Figure 7. Computed local shear rate in a vertical plane for a clearance ratio of 0.07 and a flow behavior index of 0.469 at a rotational speed of 2.5 revolutions per second at (a)  $\theta = 0^\circ$ , (b)  $\theta = 90^\circ$ , and (c)  $\theta = 150^\circ$ .

value of 13 recommended by Metzner and Otto (1957), the value of  $K_s$  in Eq. 15 is fixed as

$$K_s = 4\pi \quad (16)$$

Following the work of Beckner and Smith (1966) and Shamlou Ayazi and Edwards (1989), a power-law type of functional

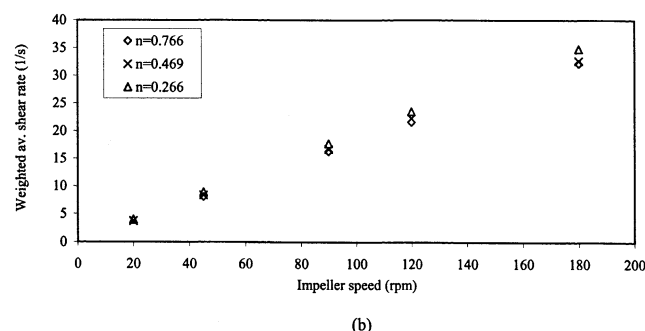
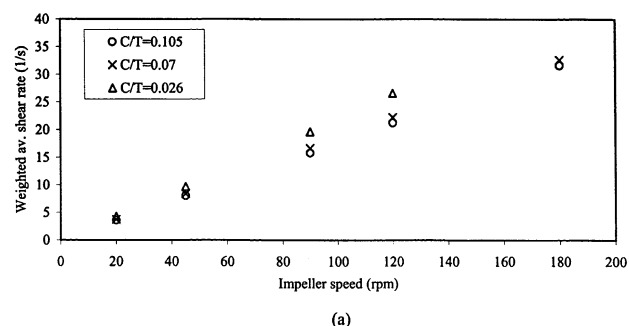


Figure 8. Variation of the weighted average shear rate near the impeller with the rotational speed (a) for various values of clearance ratio for a flow behavior index of 0.469; (b) for different values of flow behavior index for a clearance ratio of 0.070.

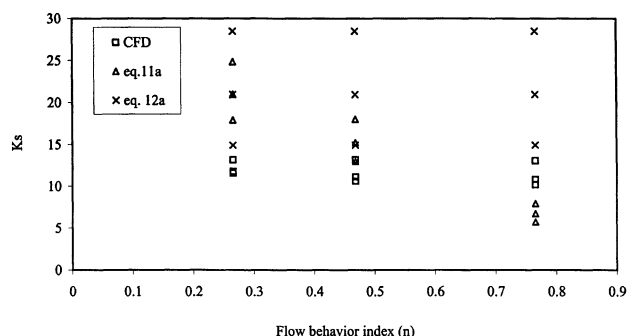


Figure 9. Variation with the flow behavior index of the  $K_s$  obtained from the present CFD computations (triangles) with those obtained empirically from the correlations of Beckner and Smith (1966) (asterisks) and Shamlou Ayazi and Edwards (1989) (open circles) for different values of clearance ratios.

dependence is sought for the clearance ratio, that is,  $Po \sim (c/T)^a$ , where the exponent  $a$  would be determined by curve-fitting. Finally, other geometric parameters such as the width and height of the blade will also have an effect on the power. This dependence is encapsulated in Eq. 7, showing that the torque required for turning the impeller, and, hence, the power, depends on the surface area of the impeller as well as on the mean radial distance from the axis of the impeller. Therefore, a dimensionless geometric factor,  $G$ , defined as

$$G = (w/d)(h/d)(d_{\text{avg}}/d), \quad (17)$$

where  $d_{\text{avg}} = (d - w/2)$ , the mean diameter of the impeller, is used to account for these variables. Thus, a correlation of the form

$$Po = C_1(d^2N^{2-n}\rho/K(4\pi)^{n-1})^{-1}(G)(c/T)^a \quad (18)$$

is sought. This correlation should work for both Newtonian and power-law fluids, as the definition of the Reynolds number in Eq. 18 reduces to that for a Newtonian fluid for all values of  $K_s$ . Using the numerical data for the Newtonian simulations alone, the values of  $C_1$  and  $a$  were found to be 372 and  $-0.6$ , respectively. Thus, the final correlation for the power consumption can be written as

$$Po = 372 \left[ d^2 N^{2-n} \rho / K (4\pi)^{n-1} \right]^{-1} (w/d)(h/d) \times [(d - 0.5w)/d](c/T)^{-0.6} \quad (19)$$

A comparison between the  $Po$  predicted using the correlation just given and that predicted by CFD for the 70 cases of Newtonian and power-law fluids simulations considered in the present study is shown in Figure 10. Also shown here are the predicted values using the correlations of Beckner and Smith (1966) and of Shamlou Ayazi and Edwards (1989). It can be seen that the predictions of Eq. 19 are as good as those of

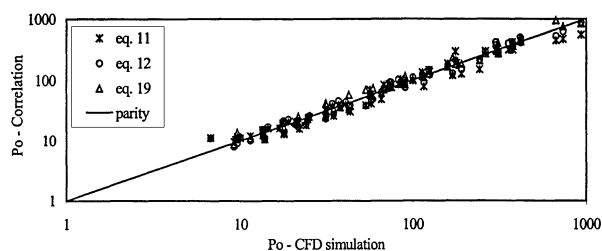


**Figure 10. Power number predicted by Eqs. 11, 12 and 19 vs. that obtained directly from the CFD simulations.**

the literature correlations for the present numerical data. This shows that a constant  $K_s$  value can be used along with the Metzner–Otto concept to correlate the data of power for anchor impellers. It should be noted that the two empirical constants involved in Eq. 19, namely,  $C_1$  and  $a$ , have been derived from *Newtonian* fluid simulations only. The good agreement in Figure 11, therefore, constitutes *direct* proof of the validity of the Metzner–Otto concept for anchor impellers.

As a final and independent verification, the present correlation was tested against *data* from the literature. Although several correlations have been reported in the literature, very few data actually can be recouped from these publications because only the final, processed data, unusable in the present context, are given. Due to this, only 45 data points from Calderbank and Moo-Young (1961), with  $n$  ranging from 0.16 to 0.84 and for  $c/T$  values of 0.033 and 0.078, could be collected for testing the correlation. (It was found that in these data, there was a factor of 100 missing, that is, the reported power number values are a factor of 100 less than the actual

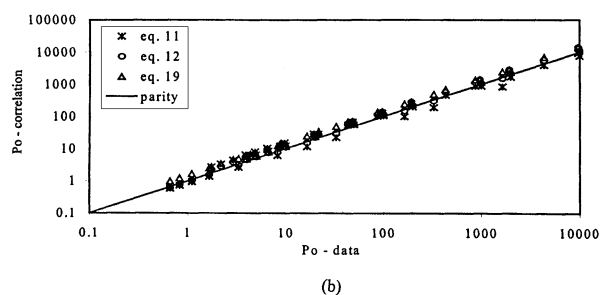
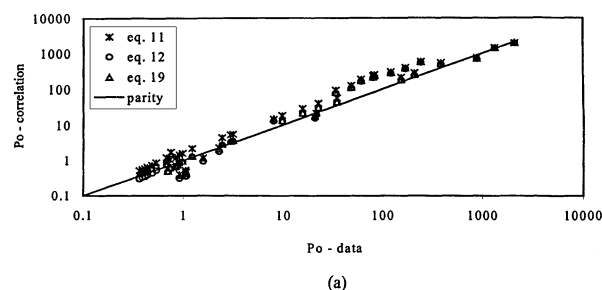


**Figure 11. Power number predicted by Eqs. 11, 12 and 19 for the data of (a) Calderbank and Moo-Young (1961), and (b) Sestak et al. (1986).**

ones. Beckner and Smith also make a passing reference to the discrepancy between their own data and those of Calderbank and Moo-Young. When the latter's data are corrected by a factor of 100, the correlations of Beckner and Smith (1966) and of Shamlou Ayazi and Edwards (1989) predicted the data remarkably accurately. This is taken as sufficient proof of the missing factor of 100). A comparison between these corrected data and the predictions of the correlations of Beckner and Smith, Shamlou Ayazi and Edwards, and the present one (Eqs. 11, 12 and 19, respectively) is shown in Figure 11a. These again show very good agreement.

Additional data were *reconstructed* from the experiments of Sestak et al. (1986), who provided correlations in the form of  $Po \cdot Re = C(n)$  for a number of systems. By setting different Reynolds number values in the range of 0.01 to 25, data could be reconstructed for different  $n$  in the range of 0.122 to 0.816 at a  $c/T$  ratio of 0.049. The comparison between these reconstructed data and the three correlations given by Eqs. 11, 12, and 19 is shown in Figure 11b. Once again, a good agreement among the three as well as with the data is found, showing that a constant  $K_s$  value of  $4\pi$  is compatible with the results as far as the power predictions are concerned.

Thus, the present correlation, based on a constant value of  $K_s$  of  $4\pi$ , can be said to be as effective as those of Beckner and Smith (1966) and Shamlou Ayazi and Edwards (1989) based on varying  $K_s$ .

## Conclusions

The present CFD simulations of the flow field created by anchor impellers show that good prediction of the power can be obtained using CFD simulations without introducing any empiricism into the modeling of the impeller. Geometric details of the impeller and rheological properties of the fluid are sufficient to calculate the power for a given rotational speed. This is true only for laminar flow; additional modeling is often required for turbulent-flow calculations.

An examination of the computed flow field shows that the shear rate near the impeller varies linearly with the rotational speed over a range of clearance ratio and flow behavior index. The proportionality constant in this linear relationship is found to be largely independent of either the clearance ratio or the fluid behavior index and roughly has a constant value of  $4\pi$ . This constitutes a direct verification of the Metzner–Otto concept (Metzner and Otto, 1957) for anchor impellers.

A correlation, based on the Metzner–Otto concept, has been developed for the prediction of power for anchor impellers for Newtonian and power-law fluids. The two empirical constants involved in this correlation have been deduced from Newtonian power simulations only. It is shown to predict well the data of power consumption for power-law type of fluids in the literature.

Taken together, the preceding results demonstrate the validity of the major assumptions made by Metzner and Otto (1957), namely, the proportionality between the shear rate near the impeller and the rotational speed, and that for anchor-driven impellers the proportionality constant is broadly independent of the geometric and rheological properties of the mixing system. Whether or not this would be the case for

more complicated impeller shapes, for example, a helical ribbon impeller where the shear rate has at least two significant shear-rate components (as opposed to the single component,  $\partial w/\partial r$ , for anchors) and a helical ribbon with a screw where the torque required to rotate the impeller would be acting at two different radii (corresponding to the mean radii of the ribbon and of the screw), is yet to be demonstrated and will require more studies of the type reported here.

## Acknowledgment

The numerical calculations reported here were performed using the facilities of the CFD Centre, IIT-Madras, India.

## Literature Cited

- Bakker, A., R. D. Laroche, M. H. Wang, and R. V. Calabrese, "Sliding Mesh Simulation of Laminar Flow in Stirred Reactors," *Trans. Inst. Chem. Eng.*, **75**, 42 (1996).
- Beckner, J. L., Ph.D. Thesis, Univ. of Wales, (1965).
- Beckner, J. L., and J. M. Smith, "Anchor-Agitated Systems: Power Input With Newtonian and Pseudo-Plastic Fluids," *Trans. Inst. Chem. Eng.*, **44**, 224 (1966).
- Bertrand, J., and J. P. Couderc, "Numerical and Experimental Study of Flow Induced by an Anchor in Viscous, Newtonian and Pseudo-Plastic Fluids," *Int. Chem. Eng.*, **25**, 257 (1988).
- Bird, R. B., W. E. Stewart, and Lightfoot, *Transport Phenomena*, Wiley, New York (1960).
- Calderbank, P. H., and M. B. Moo-Young, "The Power Characteristics of Agitators for the Mixing of Newtonian and Non-Newtonian Fluids," *Trans. Inst. Chem. Eng.*, **39**, 337 (1961).
- Harnby, N., M. F. Edwards, and A. W. Nienow, *Mixing in the Process Industries*, Butterworths, London (1985).
- Harvey, A. D., S. P. Wood, and D. E. Leng, "Experimental and Computational Study of Multiple Impeller Flows," *Chem. Eng. Sci.*, **52**, 1479 (1997).
- Kaminoyama, M., F. Saito, and K. Kamiwano, "Numerical Analysis of Mixing Processes for High-Viscosity Pseudoplastic Liquids in Mixers With Various Plate-Type Impellers," *Int. Chem. Eng.*, **33**, 506 (1993).
- Metzner, A. B., and R. E. Otto, "Agitation of Non-Newtonian Fluids," *AIChE J.*, **3**, 3 (1957).
- Murthy, J. Y., S. R. Mathur, and D. Choudhury, "CFD Simulation of Flows in Stirred Tank Reactors Using a Sliding Mesh Technique," *Inst. Chem. E. Symp. Ser. No. 136*, 341 (1994).
- Nagata, S., *Mixing—Principles and Applications*, Kodansha, Tokyo, Japan (1975).
- Peters, D. C., and J. M. Smith, "Fluid Flow in the Region of Anchor Agitator Blades," *Trans. Inst. Chem. Eng.*, **45**, 360 (1967).
- Pollard, J., and T. A. Kantyka, "Heat Transfer to Agitated Non-Newtonian Fluids," *Trans. Inst. Chem. Eng.*, **47**, 21 (1969).
- Rhie, C. M., and W. L. Chow, "Numerical Study of the Turbulent Flow Past an Airfoil with Trailing Edge Separation" *AIAA J.*, **21**, 1527 (1983).
- Rieger, F., and V. Novak, "Power Consumption of Agitators in Highly Viscous Non-Newtonian Liquids," *Trans. Inst. Chem. Eng.*, **51**, 105 (1973).
- Schilo, D., "Lietstungbedarf von Tangentialrührern beim Rustvon nicht-Newtonschem Flüssigkeiten," *Chem-Ing. Tech.*, **41**, 253 (1969).
- Sestak, J., R. Zitny, and M. Houska, "Anchor-Agitated Systems: Power Input Correlation for Pseudoplastic and Thixotropic Fluids in Equilibrium," *AIChE J.*, **32**, 155 (1986).
- Shamlou Ayazi, P., and M. F. Edwards, "Power Consumption of Anchor Impellers in Newtonian and Non-Newtonian Liquids," *Chem. Eng. Res. Des.*, **67**, 537 (1989).
- Tanguy, P. A., R. Lacroix, F. Bertrand, L. Choplin, and E. Brito-de La Fuente, "Finite Element Analysis of Viscous Mixing with Helical Ribbon Screw Impeller," *AIChE J.*, **38**, 939 (1992).
- Tanguy, P. A., F. Thibault, and E. Brito-de la Fuente, "A New Investigation of the Metzner-Otto Concept for Anchor Mixing Impellers," *Can. J. of Chem. Eng.*, **74**, 222 (1996).
- Xu, Y., and G. McGrath, "CFD Predictions of Stirred Tank Flows," *Trans. Inst. Chem. Eng.*, **74**, 471 (1996).

Manuscript received Jan. 7, 2002, and revision received Apr. 26, 2002.